Acta Neuropathologica Communications

RESEARCH

Open Access

Amplification of seeding-competent tau aggregates by PMCA in human and experimental tauopathies

Florian Almela[1,2†], Maxime Belondrade[1,2†], Raphaelle Caillierez[3], Sarah Leclercq[3], Thomas Bouillet[3], Séverine Bégard[3], Marie Oosterlynck[3], Sabiha Eddarkaoui[3], Susana Boluda[4], Luc Buée[3*], Simon Nicot[1,2†], Morvane Colin[3†] and Daisy Bougard[1,2*†]

Abstract

Tau assemblies, associated with tauopathies, are believed to self-propagate through prion-like mechanisms in the central nervous system, driving neurodegeneration. Recently, protein seed amplification assays have emerged as highly sensitive methods for detecting trace amounts of misfolded protein assemblies across various neurodegenerative diseases. In this study, we utilized protein misfolding cyclic amplification (PMCA) to demonstrate that tau assemblies from the brains of transgenic mice or human patients with tauopathies can be efficiently amplified. Amplification was achieved using complex matrix substrates, such as brain homogenates or cell lysates expressing aggregation-prone mutant tau proteins, with heparin as a cofactor. This assay enabled the highly sensitive detection of tau assemblies, even at 1-million-fold dilutions of brain homogenate from aged and symptomatic THY-Tau30 transgenic mice (a model of tauopathy) and human cases of frontotemporal lobar degeneration (FTLD-*P301L*). Tau assemblies from Alzheimer's disease (AD) patients were also successfully amplified, albeit with lower sensitivity compared to other tauopathies. Critically, the PMCA-generated tau assemblies retained seeding competence, inducing further tau aggregation in reporter tau "biosensor" cells and in young THY-Tau30 mice following intracerebral injection. Together, our findings establish PMCA as an in vitro model for studying the seeded aggregation of tau assemblies, providing a powerful tool to advance research into tau aggregation mechanisms and the development of therapeutic interventions.

Keywords Tau, PMCA, Prion, Seed amplification, FTLD, Alzheimer's disease

†Florian Almela and Maxime Belondrade contributed equally to this work.

†Simon Nicot, Morvane Colin and Daisy Bougard contributed equally to this work.

*Correspondence:
Luc Buée
luc.buee@inserm.fr
Daisy Bougard
daisy.bougard@efs.sante.fr

[1]Laboratoire TransDiag, Etablissement Français du Sang, Montpellier, France
[2]Institute for Neurosciences of Montpellier, Univ Montpellier, INSERM, EFS, Montpellier, France
[3]UMR-S1172 Lille Neuroscience & Cognition (LilNCog), University of Lille, Inserm, CHU Lille, Lille, France
[4]Department of Neuropathology, DMU Neuroscience, AP-HP, Paris Brain Institute-ICM, Inserm, CNRS, Hôpital de la Pitié Salpêtrière, Sorbonne University, Paris, France

Introduction

In Alzheimer's disease (AD) and related neurodegenerative tauopathies, the microtubule-associated tau protein misfolds into self-replicating assemblies that spread throughout the brain and promote disease progression. Different tauopathies are characterized by distinct clinical symptoms and neuroanatomical distribution of tau filamentous inclusions. Tau pathology usually begins in a disease-specific brain location and then spreads through brain networks in a predictable pattern [1]. It is generally hypothesized that the spreading of tau pathology follows a prion-like seeded aggregation mechanism that involves a structural corruption of tau monomers by preformed tau seeds, resulting in newly formed tau assemblies [2]. In this context, tau seeds refer to misfolded, aggregation-prone tau assemblies that template the conversion of native tau into pathological aggregates. These seed-competent species are believed to drive the spread of tau pathology across brain regions, making them central to disease progression in tauopathies. Their capacity to induce and amplify aggregation also underpins ultrasensitive seed amplification assays, underscoring their promise as diagnostic biomarkers for tauopathies. At the molecular level, cryo-electron microscopy (cryo-EM) studies have revealed different structures of brain-derived tau filaments associated with different tauopathies [3–5]. These findings support the view that a conformational diversity or "strains" of tau aggregates underlie different tauopathies.

In the adult human brain, six tau isoforms are expressed through alternative mRNA splicing of a single *MAPT* gene. These isoforms differ by the inclusion or exclusion of two exons encoding sequences near the N-terminus of the protein (exons 2 and 3) and one exon encoding an additional microtubule-binding repeat near the C-terminus (exon 10). This results in the production of three tau isoforms with four microtubule-binding repeats (4R) and three isoforms with three repeats (3R). Notably, the relative proportions of 3R and 4R tau isoforms that are recruited into tau aggregates vary among tauopathies. For example, AD and chronic traumatic encephalopathy (CTE) are characterized by tau aggregates composed of both 3R and 4R tau isoforms (3R/4R tau pathology). In contrast, Pick's disease (PiD) is associated with the aggregation of mainly 3R tau isoforms (3R tau pathology) whereas progressive supranuclear palsy (PSP) and corticobasal degeneration (CBD) are mainly associated with the aggregation of 4R tau isoforms (4R tau pathology). Mutations in *MAPT* can also give rise to different tauopathies called frontotemporal lobar degeneration (FTLD-*MAPT*) with filamentous tau inclusions that, depending on the mutation, are made of either 3R, 4R or both 3R/4R tau. Mutations of amino acid P301 (P301S, P301L, P301T) are the most common FTLD-*MAPT* mutations and cause pure 4R tauopathies [6, 7].

Recently, in vitro proteopathic seed amplification assays (SAAs) that were adapted from the prion field have emerged as ultrasensitive methods for monitoring the self-seeding activity of a variety of misfolded protein aggregates, including alpha-synuclein [8–11], tau [12–15] and TDP-43 [16, 17]. Due to their amplification power, these assays have immediate clinical applications for early diagnosis and therapeutic developments but also have the potential for being used as research tools by providing mechanistic insights into protein seeding processes. Two distinct SAAs are currently largely used: real-time quaking induced conversion (RT-QuIC) and protein misfolding cyclic amplification (PMCA). Both techniques rely on a similar concept of cyclic recruitment of monomers onto pre-existing assembly template (seed) resulting in fibril elongation followed by fragmentation generating further templates in an autocatalytic fashion. The major differences between RT-QuIC and PMCA lie in the monomer substrate nature (recombinant vs. brain- or cell-derived) and the mode of fibril fragmentation (shaking vs. sonication). Consequently, the products of RT-QuIC and PMCA reactions are biophysically and biologically different and it is noteworthy that for prions the RT-QuIC products are not transmissible to animals [18, 19] while PMCA produces transmissible aggregates that retain strain properties in rodents [20–22]. In the case of tauopathies, successful in vitro amplification of tau aggregates across different tauopathies and in various biospecimens (brain homogenates, CSF and skin) has been achieved using RT-QuIC [12–15, 23, 24] however very little is known about the potential of the PMCA technique for the amplification of tau assemblies.

Here, we report that PMCA can efficiently amplify seeding-competent tau assemblies in vitro. We explored different sources of tau seeds, including brain-derived aggregates from a transgenic mouse model of tauopathy (THY-Tau30) [25] and human brain samples, together with various substrates and experimental conditions that enabled the sensitive amplification of tau assemblies. We provide proof-of-principle for a PMCA-based amplification of human tau seeds derived from the brains of patients with genetic forms of tauopathies (FTLD-*P301L*) or sporadic AD. We further show that the PMCA-generated tau aggregates are seeding-competent both ex vivo in tau biosensor cells [26] and in vivo following intracerebral injection in young THY-Tau30 mice. These findings indicate that PMCA can generate biologically transmissible tau assemblies and establish it as a new in vitro model to advance future research on tau aggregation.

Materials and methods

Mouse and human brain samples

Brains from wild-type and transgenic mice including (1) THY-Tau30 (generated by microinjection in C57BL/6 of the vector bearing the human tau 1N4R isoform cDNA mutated at positions P301S/G272V under the Thy1.2 promoter [25]), (2) TauKiV5 (Tau knock-in generated by insertion of the human tau1N4R P301L cDNA in the ATG locus of mouse tau [27]), (3) KO-Tau (Tau knock-out mice generated by insertion of the GFP which leads to a targeted disruption of exon one of mouse tau [28] (JAX stock #004779, Jackson)) and (4) WT C57BL/6 mice, were, after collection, rinsed in cold PBS and immediately frozen on dry ice before long-term storage at – 80 °C.

Human frontal cortex brain tissues from non-demented controls ($n = 2$), FTLD-*P301L* cases ($n = 2$) and AD patients ($n = 2$) were obtained from the Lille Neurobank and the Neuro-CEB Brainbank. Cases were anonymized, but information was provided regarding sex, age at death, and neuropathology (Supp. Table 1).

Cell culture

The stable Tau RD P301S FRET Biosensor cells (ATCC CRL-3275) and HEK293T (ATCC CRL-3216) cells were cultured in Dulbecco's modified Eagle's medium (DMEM, Gibco, 13345364) with pyruvate and without HEPES complemented with GlutaMax 1X (Gibco, 35050061), 10% foetal bovine serum (Gibco, A5256701) and 1% penicillin-streptomycin. The cells were maintained in a humidified incubator with 5% CO_2. Cell splitting was done twice a week. To generate cell substrate containing soluble 1N4R-P301L human tau, HEK293 cells were transduced by lentiviral vectors (LV) encoding 1N4R-P301L or 1N4R wild-type human tau isoforms as previously described [29, 30]. Briefly, HEK293 cells were seeded on 6-well plates and infected by LV vectors encoding h1N4R-P301L or h1N4R-WT tau. Cells were amplified post-infection and pellets from 6xT150 plates were kept at – 80 °C until use. The levels of h1N4R-P301L and h1N4R-WT tau were determined by Western blotting and ELISA as previously described [30].

Tissue homogenization

Depending on their final use, as seed or substrate, two different protocols were applied for tissue homogenization. For PMCA substrates, whole mouse brains were homogenized at 10% (w/v) in ice-cold conversion buffer (1X PBS containing 150 mM sodium chloride, 0.1% Triton, protease inhibitor cocktail EDTA-free (Roche)) in a 10 mL glass potter tissue grinder. Tissue was homogenized with 15 up and down strokes, transferred to 1.5 mL Eppendorf tubes and centrifuged at 2000 × g for 1 min at 4 °C. The supernatant was collected and aliquoted in single-experiment aliquots before freezing at – 80 °C.

For PMCA seeds, THY-Tau30 mice (at 2- and 10-months-old) and human brain homogenates were prepared at 10% (w/v) in ice-cold PBS with protease inhibitor cocktail EDTA-free (Roche). Tissues were homogenized using a high-speed homogenizer (BeadBug), transferred to 1.5 mL Eppendorf tubes and clarified at 2000 × g for 2 min at 4 °C before freezing at – 80 °C. PMCA "cell substrate" was obtained by resuspending transduced HEK293 cell pellets (the equivalent of 6 confluent T-175 flasks) in 2.5 mL of 10% (w/v) KO-Tau mouse brain homogenate, placed on a rotating wheel at 4 °C for 30 min and centrifuged at 2000 × g for 6 min. The supernatant was collected before freezing at – 80 °C in single-experiment aliquots.

PMCA assay

For PMCA reactions, brain or cell substrates prepared in conversion buffer were supplemented immediately before use with 100 µg/mL low molecular weight heparin (Sigma, H3393). Ninety µL of substrate were seeded with 10 µL of serially 10-fold diluted brain material and placed in PCR-tubes containing three Teflon beads (diameter 2.388 mm; Marteau & Lemarié). Unseeded or mock-seeded substrates were also included in each PMCA experiment as negative controls. Unless otherwise stated, one PMCA reaction (1 round) consists in 96 cycles, each cycle being composed of an incubation step (29 min 40 s) and a sonication step (20 s at ~ 150 W) at 37 °C using a Q700 sonicator (Qsonica). For serial PMCA, amplified materials were diluted 1:10 in fresh heparin-supplemented substrate and subjected to a new PMCA round. After PMCA reaction, samples were stored at -80 °C in 0.5 mL microtubes.

Enzymatic digestion of tau aggregates

Brain homogenates and PMCA samples were subjected to proteinase K (PK) or elastase (ELA) digestion to assess protease-resistant tau proteins. Samples were incubated with PK (20 µg/mL, Sigma) or ELA (2 mg/mL, Eurobio) for 30 min at 37 °C in a Thermomixer with agitation (600 rpm). For downstream Western blot analysis, reactions were stopped by denaturation of the samples at 100 °C in NUPAGE-LDS buffer (Invitrogen) containing β-mercaptoethanol. For HTRF analysis of digested samples, reactions were stopped by the addition of 2 mM phenylmethylsulfonyl fluoride (PMSF).

Immunoblotting

Brain extracts and PMCA samples were denatured at 100 °C in NUPAGE-LDS sample buffer (Invitrogen) containing β-mercaptoethanol. For undigested and digested samples, respectively ~ 10 µg total proteins and

the equivalent of ~60 µg digested proteins were run on 4–12% NUPAGE gels (Invitrogen) and electrotransferred to PVDF 0.45 µm membranes (Biorad). After a blocking step in EveryBlot Blocking solution (Biorad), Western blots were performed using ab64193 (anti-tauR1 epitope 259–266, 1:5000, Abcam), Tau5 (epitope 210–230, 1:1000, Calbiochem), 8E12 (in house antibody, 1:1000, epitope 371–389) or 7F5 (in house antibody, 1:1000, epitope 427–441) primary antibodies diluted in EveryBlot Blocking solution and incubated overnight at 4 °C. After washing in Tris-buffered saline with 0.1% Tween 20 detergent (TBST), fluorescent StarBright 520 anti-mouse or anti-rabbit were used as secondary antibodies (Biorad) for 1 h at RT. After washing in TBST, membranes were imaged dry on the imaging system ChemiDoc MP (Biorad) and analysed with Image Lab software (Biorad).

Homogenous time-resolved fluorescence (HTRF) assay

To assess the presence of tau aggregates in our samples, we used the HTRF Tau Aggregation Kit (Revvity) with low volume 96-well microplates according to the manufacturer's instructions. This assay detects human tau aggregates in brain tissues and cell cultures. HTRF was performed directly on crude brain homogenates before and after PMCA amplification. However, before HTRF analysis and depending on the samples analysed, a dilution step (1:10, 1:20, 1:30 or 1:50) was needed to obtain the best signal-to-noise ratio and/or to avoid "hook" effects. Briefly, tau aggregates were measured using a sandwich immunoassay involving an anti-tau monoclonal antibody specific for tau aggregates labelled with terbium cryptate or d2. Ten µL of diluted sample were transferred to the assay plate for the detection of tau aggregates, then 10 µL of antibody mix labelled with HTRF fluorophores were added in a single dispensing step in the 96-well plate. Plates were sealed, incubated for 20 h at room temperature and read using the Victor X4 Microplate Reader (Perkin). After excitation at 340 nm, FRET signals were measured at 665 nm and 620 nm, and the HTRF signal was expressed as the ratio of the two emission signals (665/620). Tau aggregation was expressed as %dF (delta F), defined as the percentage increase in HTRF signal relative to unseeded control samples after background subtraction. Data were analysed using GraphPad Prism software.

FRET-tau biosensor cell assay

Tau RD P301S FRET Biosensor cells and HEK293T cells were plated into a 12-well plate with 150,000 cells per well, 24 h before treatment. Sonicated Tau [244–368], also called K18 fibrils (2 µM, as prepared in [31]) were used as a positive control and PBS as negative control of the FRET assay. Serial dilutions of seed X were done in 100 µL PBS which were completed with 100 µL of Lipofectamine2000 (Life Technologies, 11668019) diluted at 1:10 in Opti-MEM (Fisher Scientific, 31985062). The transfection mixtures were incubated for 20 min at RT and gently added in the culture medium of the cells. 72 h after transfection, the cells were detached by pipetting in warm PBS. Centrifugation at 800 × g for 5 min was used to pellet the cells and to remove excess PBS. Next, Zombie NIR (fixable viability kit; BioLegend, 1:200) was added to allow exclusion of dead cells by flow cytometry. Cells were centrifuged and excess zombie NIR was removed and 500 µL warm PBS was added as a rinsing. This PBS was removed and cells were fixed in 2% paraformaldehyde (PFA) for 10 min at RT. As a final step, cells were suspended in 300 µL PBS for downstream cytometry analyses. The flow cytometer Aria SORP (BD Biosciences; acquisition software FACSDiva v7.0, BD Biosciences) with the following excitation/emission wavelengths: excitation 405 nm, CFP emission 466 ± 40 nm and FRET YFP 529 ± 30 nm; excitation 488 nm, YFP emission 529 ± 30 nm was used. The FRET data were quantified using the Kaluza analysis software v2. Results were expressed as the percentage of FRET-positive cells. For the experiments shown in Fig. 6b, measurements were obtained from three independent PMCA samples, each analysed in duplicate within three independent FRET biosensor experiments with at least 10,000 cells per replicate analysed. This resulted in a total of $n = 18$ data points per condition. A LDH assay kit was used to evaluate LDH activity released from cells according to the manufacturer's instructions (Cytotoxicity Detection Kit; Roche Applied Science, Meylan, France). Triton X-100 was used as a positive control to induce 100% of cell death. Culture media were collected and centrifuged at 250 × g for 10 min. The LDH activity was determined from the supernatant (absorbance at 490 nm) and the % of cell viability expressed as percentage relative to triton-treated cells.

Stereotaxic injections, tissue processing and immunohistochemistry

One-month-old anesthetized THY-Tau30 mice were submitted to stereotaxic intra-hippocampal bilateral injections at the bregma coordinates: posterior AP: -2.5, midline ML: – 1 and +1 and vertical depth DV: – 1.8 with the products of a cell-based PMCA reaction seeded with a 10^{-7} dilution of seed X in HEK293-Tau-P301L cell lysate supplemented with KO-Tau mouse brain homogenate with or without PMCA or the cell substrate alone subjected to 96 PMCA cycles.

One month later, THY-Tau30 mice were deeply anesthetized and trans-cardially perfused with ice-cold 0.9% saline solution, then with 4% PFA for 10 min. The brains were immediately removed, fixed overnight in 4% PFA, washed in PBS, placed in 20% sucrose for 16 h, and frozen

in isopentane until further use. Free-floating coronal Sect. (40-µm thickness) were obtained using a cryostat microtome and next used for immunohistochemistry. Non-specific binding was blocked by using "Mouse in Mouse" reagent (1:100 in PBS; Vector Laboratories). Brain slices were next incubated with the primary monoclonal biotinylated antibodies MC1 (1:1000, Peter Davies' lab) or AT8 (1:500, ThermoFisher Scientific) in PBS containing 0.2% Triton X-100, 16 h at 4 °C. The next day, slices were incubated with biotinylated anti-mouse secondary antibody (1:400, Vector Laboratories). Labelling was amplified by incubation with the avidin-biotin-HRP complex (ABC kit, 1:400 in PBS, Vector Laboratories) prior to addition of diaminobenzidine tetrahydrochloride (DAB, Sigma) in Tris-HCl 0.1 mol/L, pH 7.6, containing H_2O_2 for visualization. Brain sections were mounted, air-dried, steadily dehydrated, cleared in toluene, and cover-slipped with VectaMount (Vector Laboratories). Mounted brain sections were analysed blindly using stereology software (Mercator image analysis system, Explora Nova). Threshold was established manually to present a minimum background and remained constant throughout the analysis. The number of detected objects was related to the surface area. The region defined as quantification zone is CA1 from bregma – 1.9 to bregma – 2.9 (based on the Mouse Atlas, George Paxinos and Keith B.J. Franklin, Second Edition, Academic Press).

Statistical analysis

Statistical analysis was performed using GraphPad Prism software. P values were determined using two-way ANOVA tests. Differences were considered to be statistically significant when $p < 0.05$. For the FRET biosensor cell assay and the in vivo assay, the Shapiro-Wilk test was performed to assess the normality, after which a Kruskal-Wallis, non-parametric test was applied.

Results

Biochemical characterization of tau aggregates in THY-Tau30 mice

In our initial attempts to develop a PMCA-based tau amplification assay, we used the THY-Tau30 (Tau30) transgenic mouse model of tauopathy expressing human tau protein (1N4R isoform) bearing two pathogenic mutations (P301S and G272V) [25]. These mice develop age-dependent brain atrophy, progressive motor impairment, neurofibrillary tangles and decreased survival. Because PMCA reactions are carried out in a complex matrix of crude brain homogenate, which is not compatible with the use of fluorescent amyloid dyes like thioflavin T, we first looked for biochemical readouts of tau aggregation in brain homogenates. We evaluated two different readouts of tau aggregation in brain homogenates of Tau30 mice, which consisted of an immunoblot assay after enzymatic digestion to identify protease-resistant tau fragments (tau^{res}) and of a commercially available tau aggregation assay based on homogeneous time resolved fluorescence (HTRF) detection (Revvity).

First, the protease resistance of tau aggregates was evaluated from Tau30 brain homogenates by denaturing Western blot and using multiple anti-tau antibodies (Fig. 1a), an approach previously described for the characterization of human tau aggregates [32]. We compared brain homogenates from 2-months-old mice (prior to tau lesion onset) versus 10-months-old mice (advanced tau lesions) and tested two different proteases, elastase (ELA) (Fig. 1b) and proteinase K (PK) (Supplementary Fig. 1). Both proteases generated tau^{res} fragments from Tau30 mouse brain homogenates that were detected with the Ab64193 antibody (epitope 259–266; belonging to the microtubule-binding repeat domain (MTBR) 1 (R1) (Fig. 1a)). Since the patterns of the tau^{res} fragments obtained with both enzymes were similar, we continued the study with elastase only. The comparison of 2- versus 10-months-old Tau30 mice revealed that ELA-generated tau^{res} fragments (between 10 and 25 kDa) are abundant in 10-months-old mice while very low levels of tau^{res} fragments can be detected after immunoblots overexposure in 2-months-old mice (Fig. 1b). Because these fragments were not detected in the wild-type mouse brain homogenate (C57BL/6), it suggests that they are derived from human tau which is expressed in Tau30 mice. We next performed epitope mapping of the tau^{res} fragments using additional anti-tau antibodies (Tau5, 8E12 and 7F5) which recognize epitopes in the proline-rich region upstream of the MTBR (Tau5), directly downstream of the R4 domain (8E12) or near the C-terminus (7F5) (Fig. 1a). Among them, only 8E12 could detect some tau^{res} fragments in aged Tau30 mice (Fig. 1b) suggesting that the elastase-resistant core of tau is mostly centred around the MTBR but also extends further downstream of the R4 domain. Together, these data demonstrate that Western blot analysis after proteolysis, i.e., to generate protease-resistant tau^{res} fragments, can be used as a readout of tau aggregation in the Tau30 model.

Subsequently, we analysed the tau aggregates in Tau30 mice brain homogenates by using the HTRF-based detection kit without protease treatment (Fig. 1c). In this assay, tau aggregates are measured using an immunoassay involving anti-tau monoclonal antibodies labelled with two different fluorophores. A HTRF signal was detected in 10-months-old mice but not in 2-months-old mice ($n = 6$ mice for each age), suggesting that this assay can detect disease-associated tau species that accumulate with aging in Tau30 mice. The specificity of the signal was validated using KO-Tau and wild-type mouse brain homogenates as controls. Further, ELA treatment of 10-months-old Tau30 mouse brain homogenate prior to

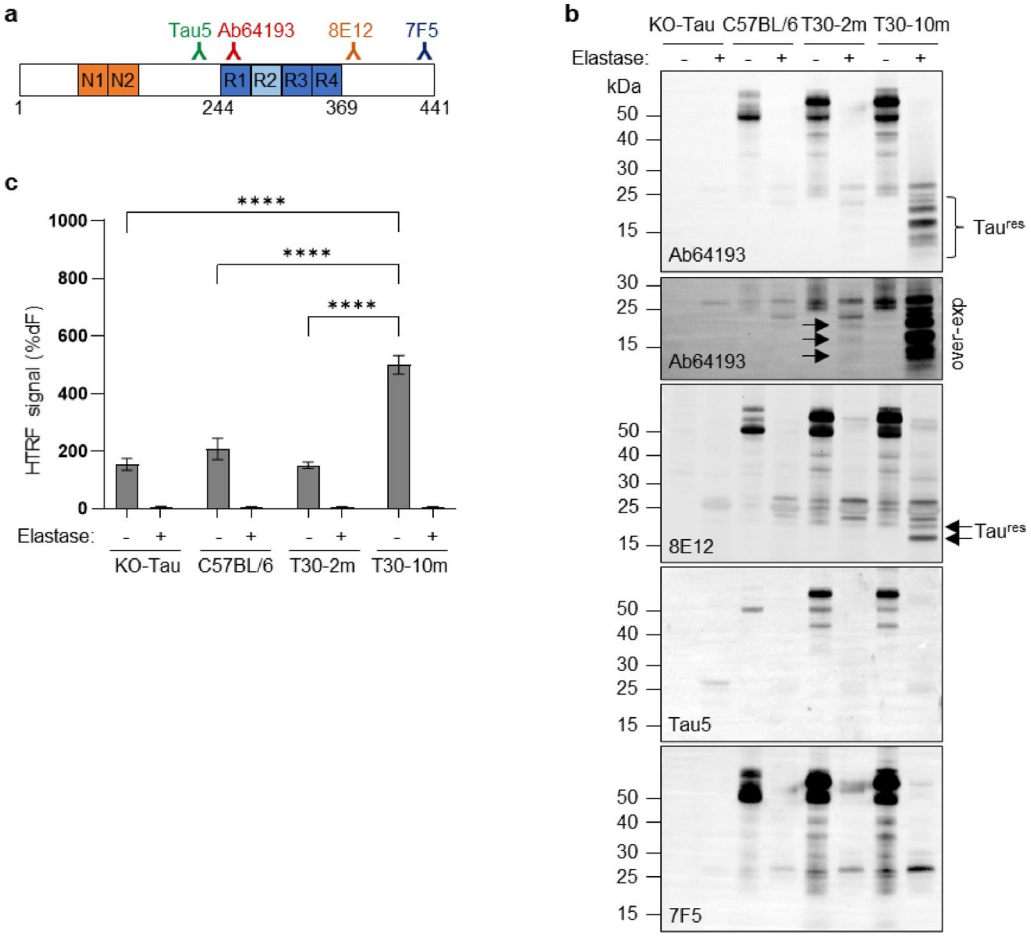

Fig. 1 Molecular characterization of tau aggregates in the Tau30 model. **a** Schematic representation of the epitopes targeted by the anti-tau antibodies included in this study (human 2N4R tau numbering): Tau5 (210–230), Ab64193 (259–266), 8E12 (371–389) and 7F5 (427–441). **b** Immunoblots of brain extracts from different mouse lines (KO-Tau, C57BL/6, Tau30 at 2- or 10-months-old) before or after elastase digestion using four different anti-tau antibodies. **c** HTRF-based detection of tau aggregates in different brain homogenates (KO-Tau, C57BL/6, Tau30 at 2- or 10-months-old) before or after elastase digestion (mean ± SD; $n = 6$ biological replicates). ****$p < 0.0001$

HTRF analysis completely abolished the signal. This suggests that the anti-tau antibodies present in the HTRF kit do not recognize the tau^{res} fragments previously identified by immunoblot. Overall, the complementarity of both types of readouts allows for the monitoring of tau assemblies formation during aging in the Tau30 mouse and in PMCA reactions.

PMCA accelerates tau aggregation in vitro in Tau30 mouse brain homogenate

To test whether PMCA can accelerate the aggregation of tau in the Tau30 model, we first performed PMCA auto-aggregation experiments (without addition of exogenous seeds) using brain homogenates from either 2- or 10-months-old Tau30 mice (Fig. 2). After 96 cycles of sonication-incubation, we observed a clear increase in the tau HTRF signal in 10-months-old Tau30 brain homogenates, but also to a lesser extent in 2-months-old Tau30 brain homogenates (Fig. 2a). These results were confirmed by immunoblot analysis after ELA digestion (Fig. 2b), showing the presence of ELA-resistant tau^{res} fragments in PMCA-treated Tau30 mouse brain homogenates. Together, these data show that sonication-incubation cycles induce the *de novo* formation of tau aggregates in vitro. Notably, the PMCA-induced tau aggregation in Tau30 mice required the addition of heparin as a cofactor. The sonication process was instrumental in accelerating tau aggregation as shown in control samples in which sonication was replaced by shaking (shaking condition), or only incubation at 37 °C (standing condition), even in the presence of heparin. As expected, time-course experiments showed a progressive increase in tau aggregation as a function of PMCA cycle numbers and also confirmed the higher levels of tau aggregates generated in 10-months-old versus 2-months-old Tau30 brain homogenates (Fig. 2c). This last observation could reflect the presence of preformed tau aggregates in 10-months-old Tau30 brain homogenates that have the capacity to seed

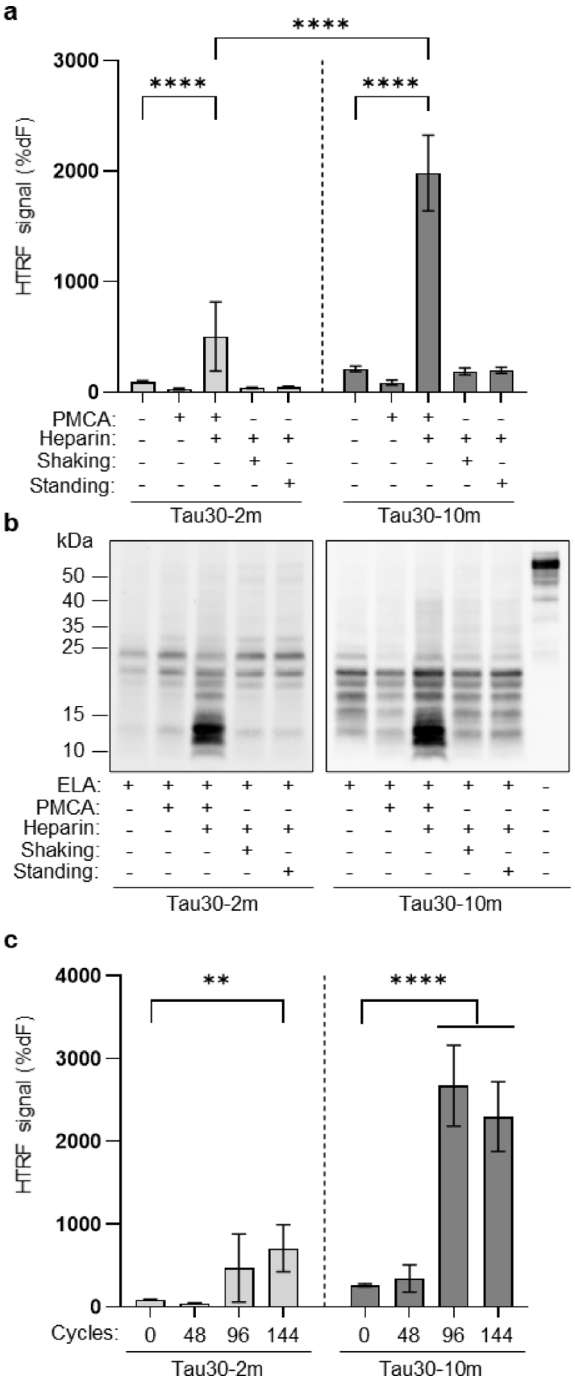

Fig. 2 PMCA sonication-incubation cycles accelerate tau aggregation in Tau30 brain homogenates. **a** HTRF-based detection of tau aggregates in Tau30 brain homogenates at 2- or 10-months-old before or after 96 PMCA cycles (with or without heparin as a cofactor) in comparison to shaking and standing controls (mean ± SD; $n = 12$ biological replicates). ****$p < 0.0001$. **b** Representative immunoblots of ELA-resistant tau species (Ab64193 antibody) generated in (a). **c** Kinetics of tau aggregation as a function of PMCA cycles number in Tau30 mice at 2- and 10-months-old ($n = 3$ biological replicates, each analysed in 2 technical replicates). **$p < 0.01$; ****$p < 0.0001$

and accelerate tau aggregation in PMCA experiments. To confirm this hypothesis, we subsequently performed seeded PMCA experiments using various sources of seeds and substrates.

Seeded amplification of tau aggregation by PMCA

As a first source of tau seeds, we used a PMCA-treated (96 cycles of sonication/incubation) brain homogenate from 10-months-old Tau30 mice, characterized by a high content of *de novo* tau aggregates. This preparation, hereafter referred to as "seed X", was used to establish the proof-of-principle for monitoring tau seeding activity by PMCA. Serial 10-fold dilutions of seed X were used to seed 2-months-old Tau30 brain homogenate substrate and the resulting mixtures were subjected to 96 cycles of PMCA. Amplified tau species were then analysed by HTRF (Fig. 3a) and immunoblot after ELA digestion (Fig. 3b). We found that seed X was highly potent at accelerating tau aggregation following PMCA in the Tau30 substrate, down to a 10^{-5} dilution (Fig. 3a, b), whereas the 10^{-2} dilution of seed X was undetectable without PMCA (i.e., frozen non-amplified dilution of seed X in PMCA substrate). Additional control experiments including mock seeding of the Tau30 substrate with seeds prepared from a KO-Tau brain homogenate, as well as a 10^{-2} dilution of seed X after PMCA using KO-Tau brain homogenate (2-months-old) as substrate remained negative under the same experimental conditions. Thus, the addition of preformed tau seed aggregates facilitates the aggregation of tau in PMCA reactions using young Tau30 brain homogenate as a substrate.

Because the Tau30 model overexpresses human tau containing two mutations (P301S and G272V), we tested other substrate sources to identify PMCA substrates less prone to spontaneous auto-aggregation. First, we tested as PMCA substrates brain homogenates from TauKiV5 mice [27] expressing physiological levels of 1N4R human tau isoform with a P301L mutation on a mouse KO-Tau background (Fig. 4a). We found that seed X efficiently triggered tau aggregation in TauKiV5 substrate after 96 cycles of PMCA (i.e., 1 round of PMCA), but only at the 10^{-2} dilution (Fig. 4b). To achieve higher sensitivity, we performed serial PMCA rounds in TauKiV5 substrate. After each round, aliquots from all reactions (corresponding to the different initial seed dilutions) were diluted 1:10 into fresh substrate and subjected to a new PMCA round. After 3 consecutive rounds of 96 cycles, we were able to detect seeding activity at the 10^{-5} dilution, indicating progressive amplification of initially low seeding levels. Importantly, non-seeded control PMCA substrates remained negative over the 3 rounds (Fig. 4b). Immunoblot analysis after ELA treatment confirmed these results, with a progressive appearance of low molecular weight tau^{res} fragments as a function of PMCA

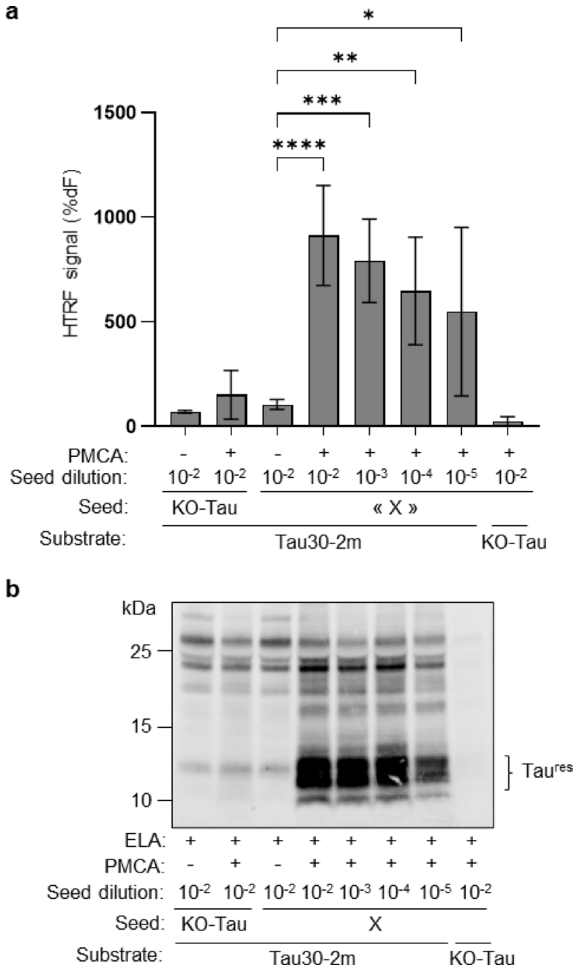

Fig. 3 Seeded amplification of tau aggregation by PMCA in young Tau30 substrate. **a** HTRF-based detection of tau aggregates before or after PMCA experiments (96 cycles) seeded with X at different dilutions in young Tau30 substrate or in KO-Tau substrate control (mean ± SD; $n = 5$ biological replicates). *$p < 0.05$; **$p < 0.01$; ***$p < 0.001$; ****$p < 0.0001$. **b** Representative immunoblots of ELA-resistant tau species (Ab64193 antibody) generated in (a). Seed X, PMCA-treated 10-months-old Tau30 brain homogenate

rounds (Fig. 4c). Thus, compared to the Tau30 substrate, the TauKiV5 substrate appears to be more stable, allowing it to be used in serial rounds of PMCA. However, the limited PMCA sensitivity obtained with this substrate (i.e., 10^{-5} dilution of seed X after 3 rounds compared to 1 round for Tau30 substrate (Fig. 3)) prompted us to look for an alternative one with higher amplification potential.

Inspired by the prion literature, we attempted to perform PMCA using cell lysates as substrates (cell-based PMCA) (Fig. 5) [33, 34]. For this purpose, we engineered stable HEK293 cells overexpressing human 1N4R tau with or without a P301L mutation. Cell-based PMCA substrates were obtained by resuspending HEK293 cell pellets in 10% (w/v) brain homogenate from KO-Tau mice in conversion buffer. This supplementation was introduced not only to increase the overall protein content [35] but also to provide biologically relevant molecules (e.g., lipids and other brain-derived components) known to influence tau aggregation and seeding efficiency. Importantly, the use of Tau knockout brain homogenate ensures that no endogenous tau seeds are introduced into the reaction. As shown in Fig. 5a, this new PMCA assay allowed the detection of seed X in dilutions as extreme as 10^{-9} and in a single PMCA round of 96 cycles. No amplification of seed X was obtained in PMCA reactions using either non-transfected HEK293 cells or HEK293 cells expressing wild-type 1N4R human tau and supplemented with KO-Tau brain homogenate as substrate. These results were confirmed by immunoblot analysis of the PMCA products after protease digestion (Fig. 5c), pointing at the P301L mutation in human 1N4R tau as a key factor for efficient seed amplification. Thus, the cell-based PMCA enables highly sensitive detection of seed-competent tau species, at least from the "artificial" seed X.

Biological characterization of newly formed tau aggregates by PMCA

To evaluate the biological activity of newly formed tau aggregates following PMCA, and more precisely to test whether the PMCA products can seed tau aggregation ex vivo, we used a cellular assay previously described by Diamond and colleagues to quantify tau aggregates in human patient samples [26]. These "biosensor" HEK293 cells express soluble forms of tau repeat domain (RD: aa244-368) containing a disease-associated mutation (P301S) fused to cyan or yellow fluorescent proteins (CFP/YFP). Exposure of these cells to seed-competent tau aggregates induces soluble tau RD-CFP/YFP nucleation that generates a fluorescence resonance energy transfer (FRET) due to the proximity of CFP and YFP that can be detected by flow cytometry.

Here, after lipofection, we incubated for 72 h the biosensor cells with serial 10-fold dilutions (titration) of the products of cell-based PMCA reactions seeded with a 10^{-7} dilution of seed X and quantified the percentage of FRET-positive cells using flow cytometry (Fig. 6a). As compared to control cells exposed to a 10^{-7} dilution of seed X without PMCA, or to cells exposed to mock-seeded cell-based PMCA reactions, we detected a specific FRET signal after seeding with cell-based PMCA amplicon dilutions (from 10^{-3} to 10^{-5}) (Fig. 6b). In parallel, cell viability assays showed almost absence of toxicity associated with PMCA amplicons at these dilutions, except for the 10^{-3} dilution showing a slight cytotoxicity (Supplementary Fig. 2). Thus, tau aggregates generated from Tau30 mice (after PMCA auto-aggregation) and subsequently amplified in a cellular substrate by PMCA can seed the aggregation of tau RD-CFP/YFP ex vivo in biosensor cells.

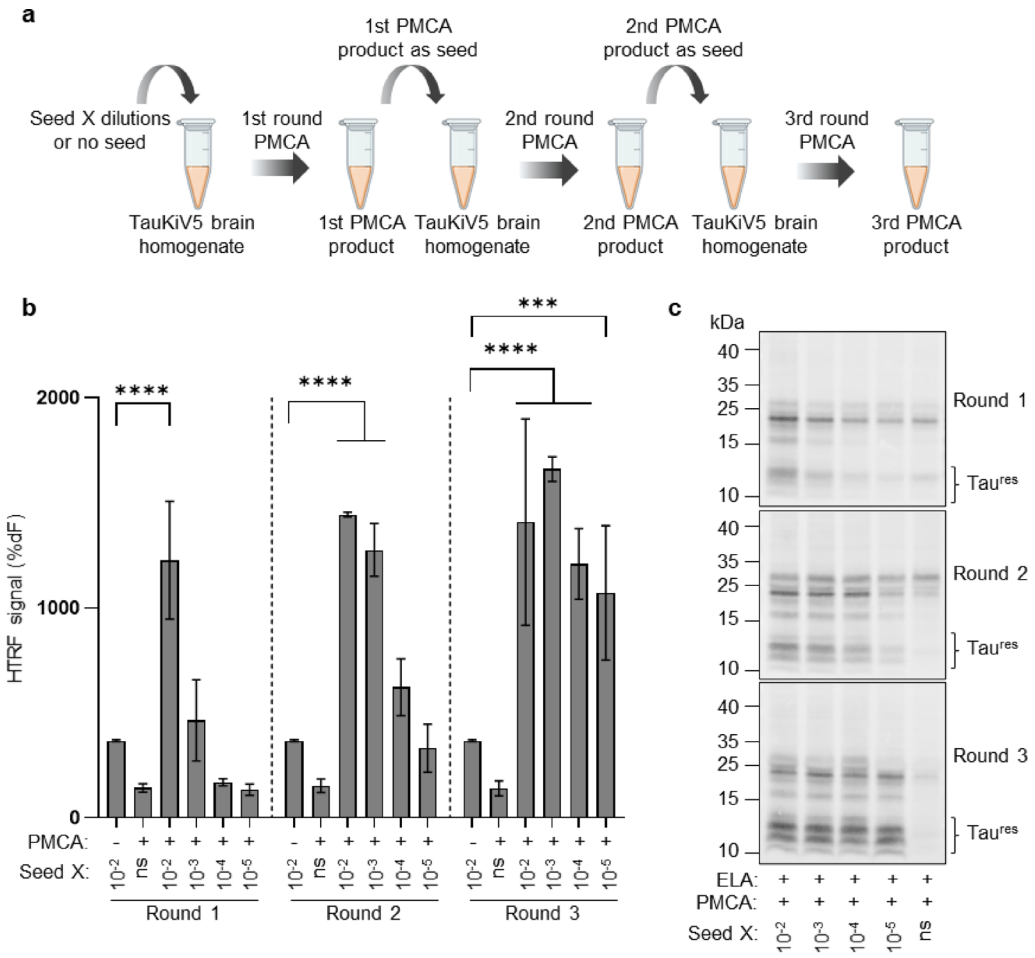

Fig. 4 Seeded amplification of tau aggregation over serial PMCA rounds in TauKiV5 substrate. **a** Schematic representation of serial PMCA. **b** HTRF-based detection of tau aggregates in TauKiV5 brain homogenate substrate seeded with X at different dilutions (mean ± SD; $n = 3$ biological replicates) during 3 consecutive PMCA rounds of 96 cycles. ***$p < 0.001$; ****$p < 0.0001$. ns, no seed. **c** Representative immunoblots of ELA-resistant tau species (Ab64193 antibody) generated in (a). Brackets on the right of each panel highlight low molecular weight ELA-resistant tau fragments specifically detected in seeded PMCA amplicons. Seed X, PMCA-treated 10-months-old Tau30 brain homogenate

Next, we investigated whether the products of PMCA reactions can also induce tau seeding in vivo in our previously described seeding model [36, 37]. Young Tau30 mice (1-month-old) were bilaterally injected into the CA1 layers of the hippocampus with the products of a cell-based PMCA reaction seeded with a 10^{-7} dilution of seed X (Fig. 6c). At this age, the endogenous tau pathology is very weak, thus allowing us to evaluate the seeding activity associated with the injected material [36]. As controls, we inoculated either the same sample but without PMCA (i.e., 10^{-7} dilution of seed X in HEK293-Tau-P301L cell lysate supplemented with KO-Tau mouse brain homogenate) or the cell substrate alone subjected to 96 PMCA cycles. Mice were sacrificed 1-month post-injection and tau lesions were examined in the brains of these animals using the well-characterized anti-tau antibody MC1 (a conformation-dependent tau antibody) [38]. MC1-positive tau lesions were observed in some pyramidal neurons of the hippocampal CA1 layer in most of the mice injected with the seed X after cell-based PMCA amplification, whereas no lesion was present in the two control mice cohorts (Fig. 6d). Immunohistochemical analysis using the phosphorylation-dependent antibody AT8 further confirmed the presence of pathological tau in the same brain regions. Quantification of the MC1 and AT8 signals confirmed that the results were statistically significant (Fig. 6e). Thus, the PMCA samples that contained tau assemblies amplified from seed X were able to seed the aggregation of tau in vivo in the neurons of young Tau30 mice.

Detection of endogenous tau seeds in Tau30 mice brain

Having shown successful amplification of seed X and characterized biologically the amplified tau assemblies, we next evaluated the presence of endogenous tau seeds in the brain of Tau30 mice by the cell-based PMCA (Fig. 7). We compared the seeding potential of 2- versus 10-months-old Tau30 mice brain homogenates ($n = 3$).

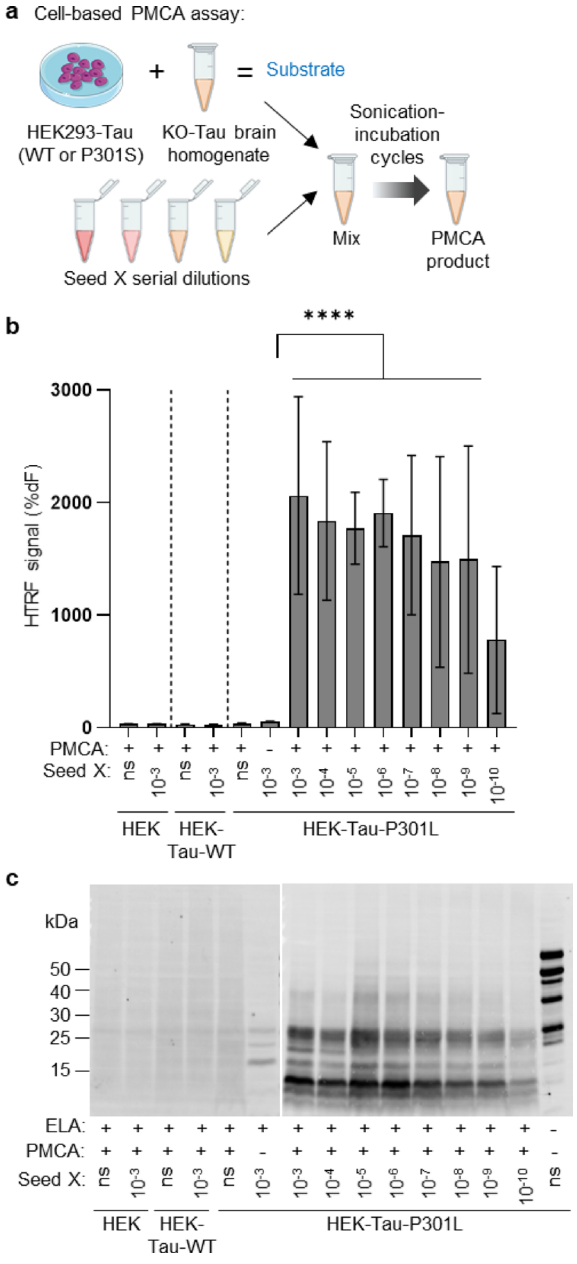

Fig. 5 Cell-based seeded amplification of tau aggregates by PMCA. **a** Schematic representation of the cell-based PMCA assay. **b** HTRF-based detection of tau aggregates in HEK293-Tau cell substrates after PMCA experiments (96 cycles) seeded with X at different dilutions (mean ± SD; $n = 5$ biological replicates). ****$p < 0.0001$. ns, no seed. **c** Representative immunoblots of elastase (ELA)-resistant tau species (Ab64193 antibody) generated in (a). Seed X, PMCA-treated 10-months-old Tau30 brain homogenate

After a first PMCA round of 96 cycles, tau seeding activity was undetectable in 2-months-old mice and very limited in 10-months-old mice (low detection of only a 10^{-4} dilution of brain homogenate) (Fig. 7b). However, prolonging the PMCA rounds led to a robust and specific detection of tau seeds in both 2- and 10-months-old Tau30 mice, with a higher sensitivity for 10-months-old mice as compared to 2-months-old mice (end-point brain homogenate dilution of 10^{-8} versus 10^{-6}) (Fig. 7a, b). Collectively these results validate the cell-based PMCA assay for the detection of endogenous tau aggregates and suggest that seed-competent tau species are formed as early as 2 months of age in this transgenic mouse model.

Tau seeding activity in brain from FTLD-*P301L* patients

To establish the proof-of-principle for a PMCA-based detection of human disease-associated tau aggregates, we tested 2 human cases of frontotemporal lobar degeneration associated with a P301L mutation (FTLD-*P301L*), thus comparable to the P301S tau mutation in Tau30 mice, and 2 controls from non-demented patients. Serial ten-fold dilutions of brain samples (frontal cortex) from patients were used as potential seeds in cell-based PMCA reactions (Fig. 8). Tau seeding activity was undetectable after a first PMCA round of 96 cycles. As previously observed for Tau30 mice, prolonging the PMCA rounds allowed the detection of a tau seeding activity from the two FTLD-*P301L* samples down to a 10^{-4} brain homogenate dilution, whereas the two control brain samples remained negative in these conditions (Fig. 8a). These data support the idea that tau aggregates from human FTLD-*P301L* brain samples are seed-competent and trigger tau aggregation in vitro in PMCA reactions. We next pre-treated the two FTLD-*P301L* brain homogenates with sonication-incubation cycles as described above to generate the seed X with 10-months-old Tau30 mice (i.e., auto-aggregation conditions), to test whether this pre-treatment could increase amplification efficiency. Pre-treated FTLD-*P301L* or control brain homogenates were then serially ten-fold diluted and each dilution mixed with fresh substrate (HEK293-Tau-P301L cell lysate supplemented with KO-Tau brain homogenate) and subjected to PMCA (Fig. 8b). We found that this pre-treatment greatly increased the specific seeding potential of both FTLD-*P301L* cases down to the detection of a 10^{-6} dilution and in a single round of cell-based PMCA.

Tau seeding activity in brain from AD patients

Finally, we tested the presence of tau seeds by cell-based PMCA in the brain of two sporadic AD patients with clinically and neuropathologically characterized features (Supplementary Table). As described above, serial ten-fold dilutions of brain samples (frontal cortex) from patients were used as potential seeds in serial cell-based PMCA reactions (Fig. 9). After 3 rounds of PMCA, we detected specific tau seeding activity in AD brain samples, within the 10^{-4} to 10^{-5} dilution range. Thus, the cell-based PMCA assay could specifically detect some tau seeding activity in AD brain samples but with lower sensitivity. As previously tested for FTLD-*P301L*, we performed a pre-treatment of brain homogenates with

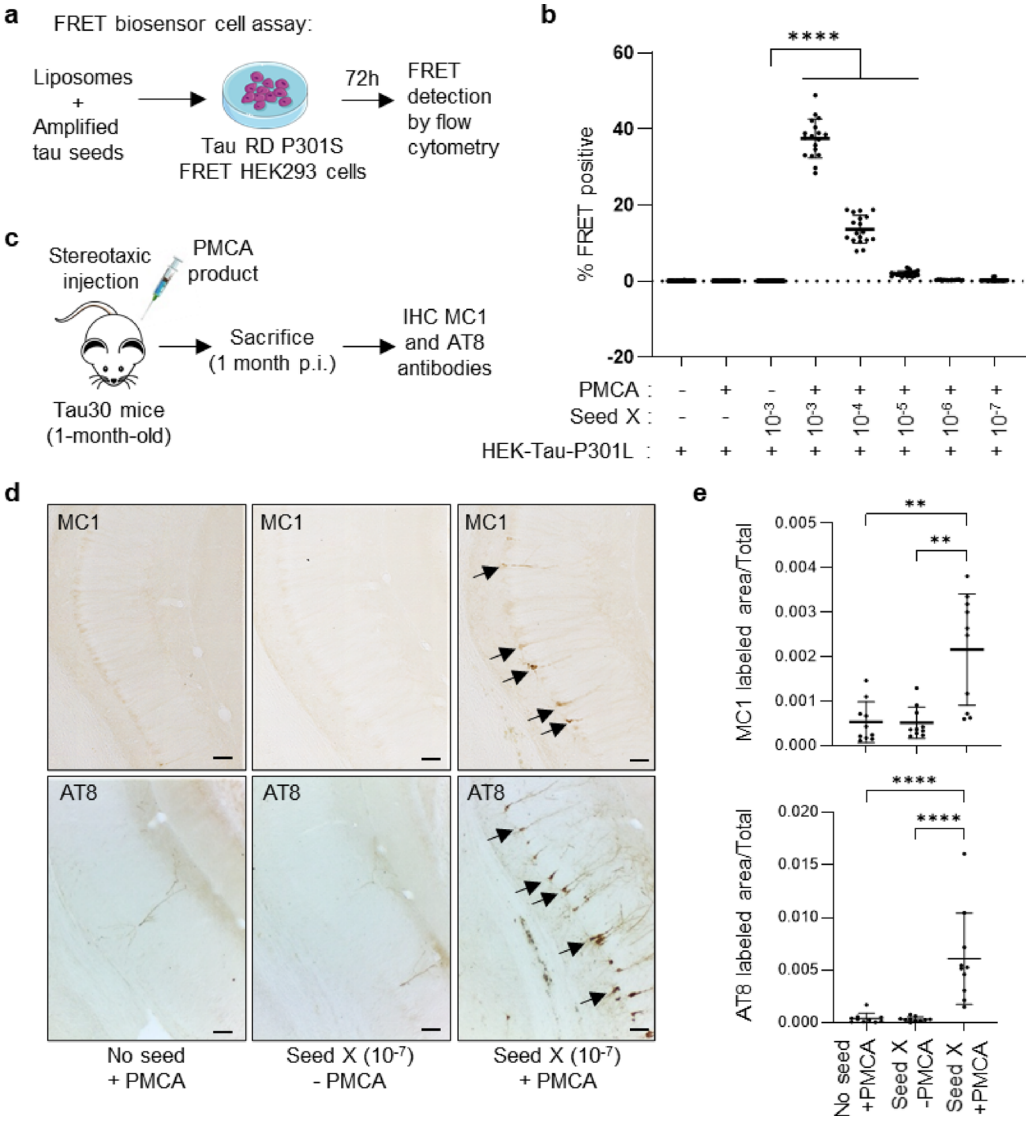

Fig. 6 Biological characterization of PMCA-amplified tau aggregates. **a** Schematic representation of the FRET biosensor assay workflow. Lipofectamine/seed complexes are applied to biosensor cells for 72 h. When successful, seeded aggregation produces a FRET signal that is measured by flow cytometry. **b** FRET biosensor titration of tau seeding activity in serial dilutions (10^{-3} to 10^{-7}) of a cell-based PMCA amplicon (10^{-7} dilution of seed X amplified in Tau-P301L substrate) versus controls. Data points ($n = 18$ per condition) were obtained from 3 independent PMCA samples, each analyzed in duplicate across 3 independent FRET biosensor experiments. ****$p < 0.0001$. **c** Schematic representation of the in vivo seeding assay workflow. Bilateral stereotaxic injections of PMCA samples are done in the hippocampus of 1-month-old Tau30 mice followed by immunohistochemistry (IHC) analysis 1 month later using a conformational anti-tau antibody (MC1) as well as a phosphorylation-dependent anti-tau antibody (AT8). p.i., post-injection. **d** IHC analysis of hippocampal brain slices from Tau30 mice injected with indicated samples and labeled with the conformational anti-tau antibody MC1 and the phosphorylation-dependent anti-tau antibody AT8. Arrows are pointed at neuronal cell bodies showing MC1 and AT8 immunoreactivity in mice injected with seed X amplified by PMCA. Scale bars, 50 µm. **e** Graphical representation of MC1- and AT8-immunoreactive areas from the in vivo seeding experiments (each dot corresponds to an individual mouse). Results are presented as MC1- and AT8-immunoreactive areas normalized to the total analyzed area. **$p < 0.01$, ****$p < 0.0001$. Seed X, PMCA-treated 10-months-old Tau30 brain homogenate

sonication-incubation cycles to assess whether tau seeding activity from AD samples could be improved. Unfortunately, we found no improvement of PMCA sensitivity for AD after pre-treatment of brain homogenates (data not shown). This revealed a marked difference between the two types of tauopathies, as FTLD-*P301L* detection was greatly enhanced after pre-treatment.

To investigate whether inter-individual variability in seeding activity could be related to differences in tau species, we performed Western blot analyses on all brain lysates (controls, FTLD-*P301L*, and AD) using antibodies against total tau and phospho-tau (Supplementary Fig. 3). These analyses did not reveal major differences in global tau profiles nor a clear correlation with PMCA efficiency.

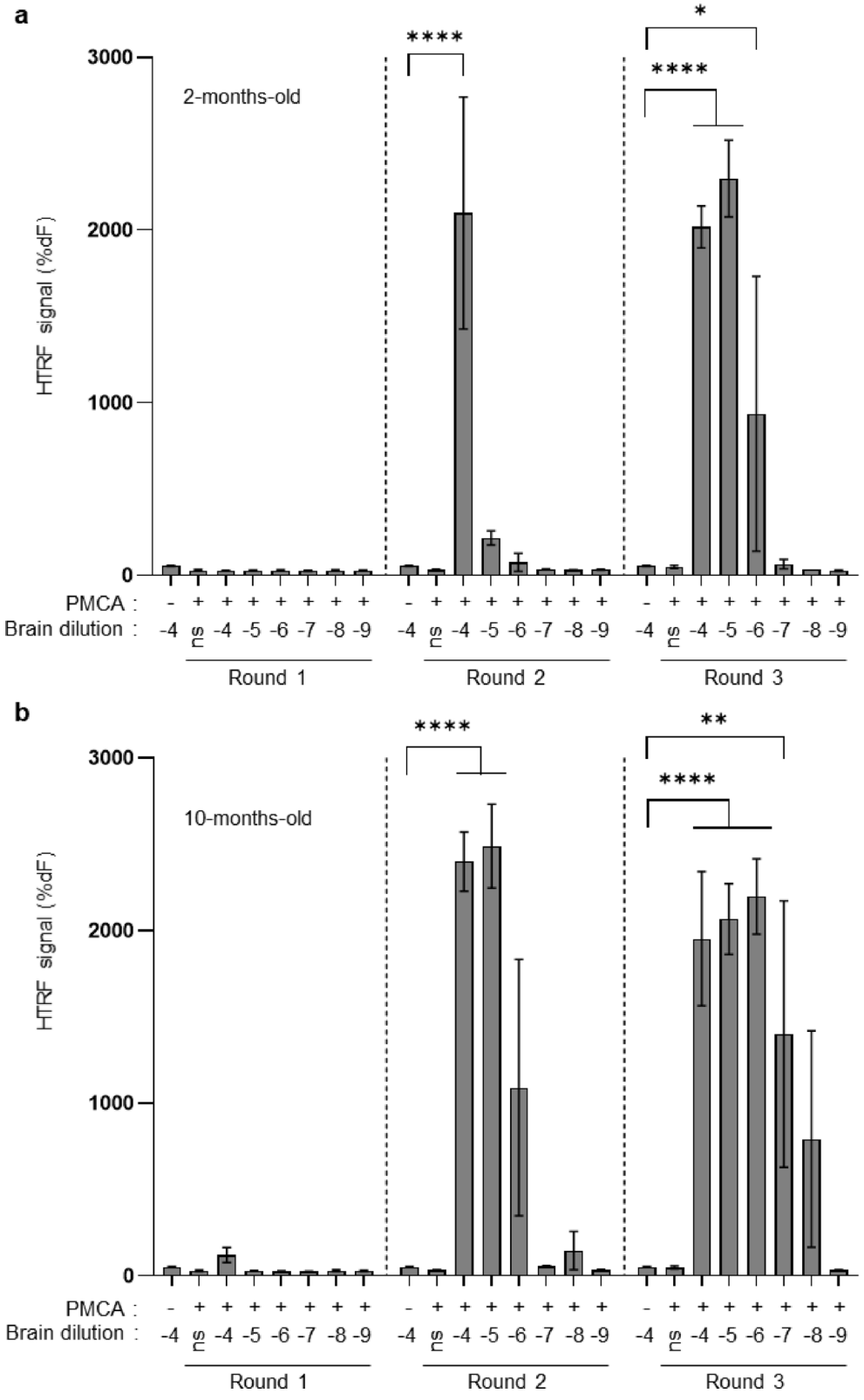

Fig. 7 Detection of endogenous tau seeding activity in the brain of Tau30 mice. HTRF-based detection of tau aggregates after cell-based PMCA experiments seeded with brain homogenates from 2-months-old (**a**) or 10-months-old (**b**) Tau30 mice at different dilutions (mean ± SD; $n = 3$ biological replicates). ns, no seed. *$p < 0.05$; **$p < 0.01$; ****$p < 0.0001$

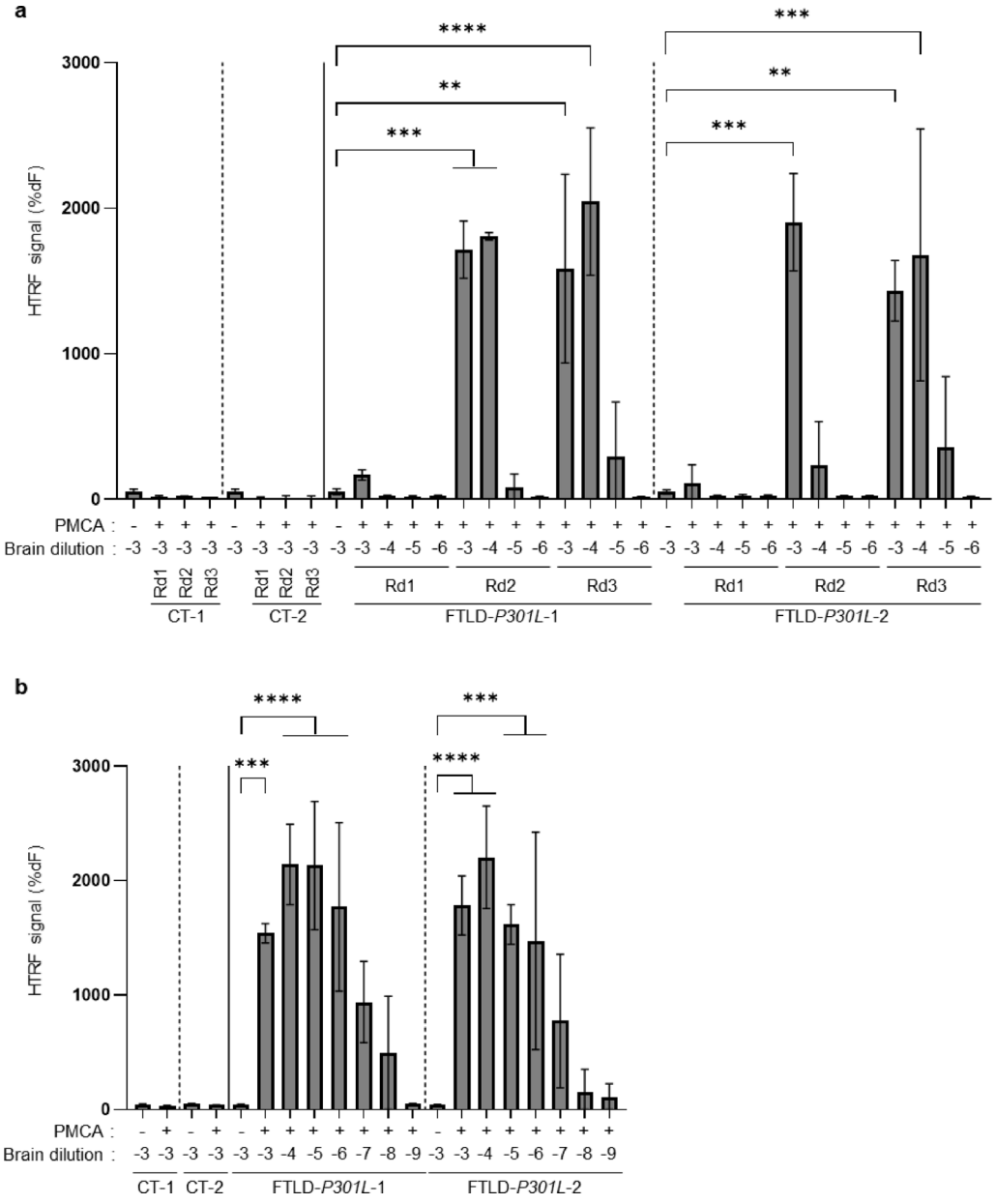

Fig. 8 Tau PMCA seeding activity in human cases of FTLD-*P301L* tauopathy. **a** HTRF-based detection of tau aggregates after cell-based PMCA experiments seeded with 10-fold dilutions of brain homogenates from two human cases of FTLD-*P301L* (FTLD-*P301L*-1 and FTLD-*P301L*-2) or two non-demented human control cases (CT-1 and CT-2) (mean ± SD; $n = 3$ technical replicates). Three consecutive PMCA rounds of 96 cycles were performed. $^{**}p < 0.01$; $^{***}p < 0.001$; $^{****}p < 0.0001$. **b** Pre-treatment of brain homogenates (96 cycles of sonication-incubation with heparin) strongly improves the seeding potential of FTLD-*P301L* brains but not controls. As in (a) tau aggregates in PMCA amplicons were detected by HTRF after cell-based PMCA experiments (mean ± SD; $n = 3$ technical replicates). Only 1 PMCA round of 96 cycles was performed. $^{***}p < 0.001$; $^{****}p < 0.0001$

Discussion

The development of sensitive protein seed amplification assays that can detect minute amounts of misfolded protein aggregates from biological specimens has become an important area of research in the field of neurodegenerative diseases. The two most common amplification assays include PMCA and RT-QuIC, which differ by the amplification substrate nature and the mode of fibril fragmentation. For tau seed amplification specifically, the vast majority of published data has been obtained with the RT-QuIC assay, using mostly fragments of 3R or 4R recombinant tau as substrates [12–15, 23, 24], but also more recently full-length tau [39–41] or a combination of both [42]. In contrast, very few studies have relied on PMCA-based assays for the seeded amplification of tau aggregates. One study has reported amplification of tau seeds by repeated cycles of sonication using recombinant tau substrates, thus combining some PMCA and

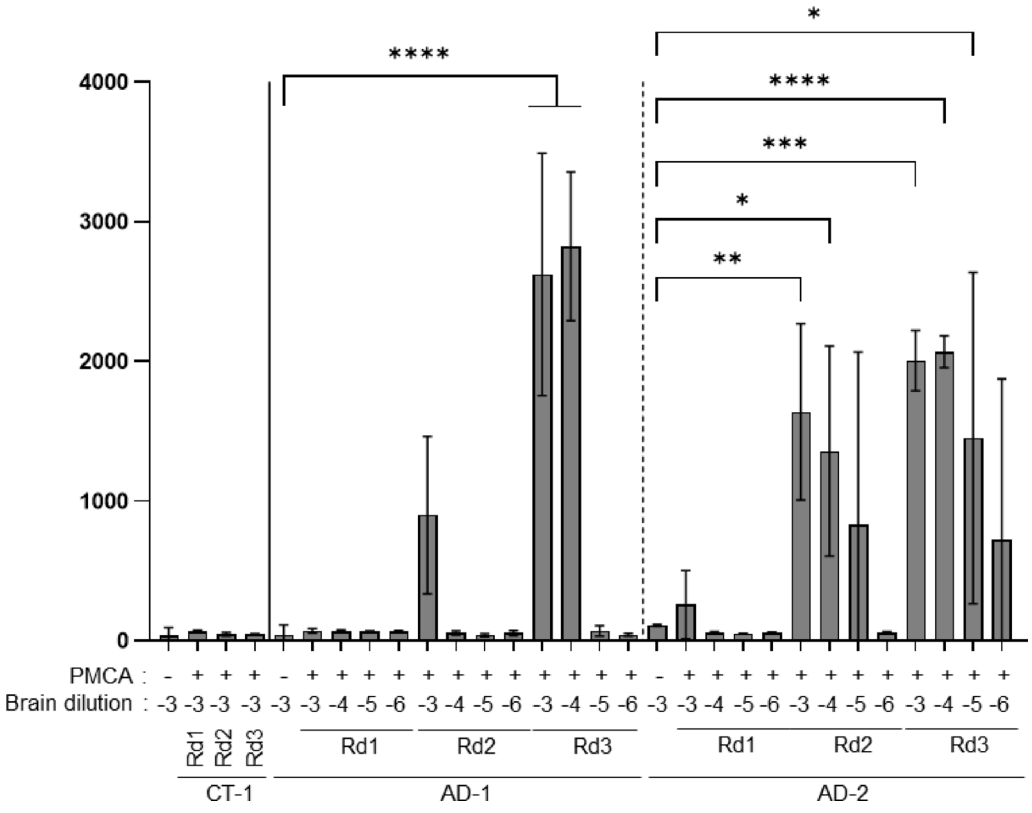

Fig. 9 Tau PMCA seeding activity in two Alzheimer's disease (AD) patients. HTRF-based detection of tau aggregates after cell-based PMCA experiments seeded with 10-fold dilutions of brain homogenates from two AD cases or one non-demented human control case (CT-1) (mean ± SD; $n = 3$ technical replicates). Three consecutive PMCA rounds of 96 cycles were performed. *$p < 0.05$; **$p < 0.01$; ***$p < 0.001$; ****$p < 0.0001$

RT-QuIC specifications [43]. However, to our knowledge, traditional PMCA assays based on brain- or cell-derived tau "biological" substrates have not been described.

Our work demonstrates that tau seeds from transgenic mice or humans with tauopathies can be efficiently amplified by PMCA in substrates derived from (i) brain homogenates from transgenic mice expressing full-length 1N4R P301S-G272V tau and (ii) cell extracts from HEK293 cells expressing full-length 1N4R P301L tau. Thus, tau seeds are the third class of protein aggregates to be amplified by PMCA after PrP [44] and α-synuclein [11] prions. However, unlike PrP and α-synuclein, tau seed amplification by PMCA strictly required the presence of a cofactor of aggregation (here heparin). This observation highlights the difficulty of inducing tau aggregation in vitro without cofactors and is consistent with previously published seeded aggregation assays [12, 14, 43] as well as tau fibrillation studies in the absence of seeds where negatively charged molecules such as heparin [45], RNA [46], or arachidonic acid [47] are generally required to induce tau aggregation in vitro. While heparin is widely used to promote tau aggregation in vitro, it is not physiologically present in the brain. The dependence on heparin observed in our PMCA conditions therefore suggests that the tau assemblies generated in this system may not fully recapitulate those formed in vivo. We also found that efficient PMCA amplification of tau seeds was achieved using aggregation-prone mutated tau substrates, either from mouse brains or cell extracts (P301S-G272V and P301L respectively). These "non-physiological" mutants are known to facilitate tau aggregation potential and it is noteworthy that cell extracts expressing wild-type 1N4R human tau substrate did not sustain seeded tau amplification by PMCA in our experiments. While the use of aggregation-prone mutant tau substrates enabled robust amplification in our system, it may represent a limitation when studying sporadic tauopathies. These mutations enhance tau aggregation propensity and may influence amplification efficiency or conformational selection. Notably, the use of aggregation-prone tau variants is widely adopted in in vivo and ex vivo seeding models to enhance sensitivity and facilitate the detection of tau seeding activity. Future studies will be required to determine to what extent PMCA amplification preserves the structural and biological properties of tau assemblies derived from different tauopathies.

Similarly to our previous report on α-synuclein PMCA [11], we have shown here that repetitive sonication-incubation cycles of Tau30 mouse brain homogenates trigger the formation of protease-resistant tau aggregates even

without the addition of exogenous seeds. Most likely, this spontaneous generation of tau aggregates implicates the aggregation-prone 1N4R mutated human tau expressed by Tau30 mice. In addition, we found higher levels of newly generated tau aggregates in 10-months-old versus 2-months-old Tau30 brain homogenates. One explanation for this observation would be the presence of higher levels of preformed seeding-competent tau aggregates in 10-months-old mice that have the capacity to seed and accelerate further tau aggregation in PMCA experiments.

The use of complex biological substrates endows PMCA with the peculiarity of generating infectious PrP prions that maintain strain properties [21]. Beyond PrP prions, amplification of α-synuclein seeds in brain homogenates and blood of transgenic mice has also been achieved by PMCA [11, 48]. The PMCA-amplified α-synuclein aggregates were shown to be transmissible to mice by intracerebral inoculation [11, 49]. Remarkably, we show here that PMCA-generated tau assemblies can induce tau aggregation both ex vivo in biosensor cells and in vivo in the brain of young Tau30 mice after intracerebral inoculation. To our knowledge, this "pathogenic activity" has not yet been described for recombinant tau fibrils obtained after RT-QuIC amplification. In future studies it will be interesting to investigate whether different tau "strains" can be efficiently amplified by PMCA and if they retain strain-specific pathogenic properties in reporter cells or mice.

Using cell-based PMCA we detected endogenous tau seeds in Tau30 mice as early as 2 months of age. Since the detection of phosphorylated tau-positive neurons and Gallyas silver-staining positive neurons start around 3 months in this model [25], it suggests a concomitant increase in seeding-competent tau species. Beyond Tau30 mice, we detected human tau seeds derived from the brains of a few patients with both genetic (FTLD-*P301L*) and sporadic (AD) tauopathies. In our experimental conditions, the detection limit was moderate in both types of tauopathies (end-point brain dilution of 10^{-4}). Unexpectedly, we found that repetitive sonication-incubation cycles of FTLD-*P301L* brain alone (but not AD) in the presence of heparin greatly enhance the PMCA seeding activity by several orders of magnitude. Most likely, this observation reflects a newly generated population of tau seeds linked to mutant P301L in the brains of FTLD-*P301L* patients, as was previously observed with Tau30 mice. While these results demonstrate that PMCA can detect tau seeding activity in both genetic and sporadic tauopathies, the present study remains limited to FTLD-*P301L* and AD cases. Further investigations will be required to determine whether PMCA can efficiently amplify tau seeds from a broader spectrum of tauopathies, including those characterized by distinct isoform composition and conformational properties such as 3R tauopathies (e.g., PiD) or other 4R tauopathies.

In comparison with PMCA, AD tau seeds can be detected by RT-QuIC in endpoint brain dilutions as low as 10^{-8} [13, 14, 41, 50]. Moreover, tau seeds from PiD and 4R tauopathies such as PSP and CBD can also be sensitively amplified by RT-QuIC using different tau substrates and experimental conditions, not only in brain tissue but also in CSF and skin samples [12, 15, 23]. Further optimizations, including the use of different tau substrate isoforms and/or specific mutations, will be required to determine whether similar detection sensitivities can be achieved with PMCA. In the future, adapting PMCA for the detection of tau seeds in additional tauopathy types and in diagnostically accessible biospecimens will be of crucial importance to extend its prospective clinical applications.

Supplementary Information

The online version contains supplementary material available at https://doi.org/10.1186/s40478-026-02345-4.

Supplementary Material 1

Acknowledgements

We are grateful to Sylvie Claeysen and the iExplore Facility (RAM, BioCampus Montpellier) for housing the KO-Tau mice. We acknowledge the Lille Neurobank (Romain Perbet and Claude-Alain Maurage) and the Neuro-CEB Neuropathology Network (Danielle Seilhean) for providing us with human samples. Neuro-CEB is supported by patient associations (Vaincre Alzheimer, France Parkinson, ARSLA, ARSEP, CSC, France DFT, PSP France, BRAIN-TEAM) and by Assistance Publique- Hôpitaux de Paris (AP-HP).

Author contributions

Conceptualization: FA, MB, LB, SN, MC, DB. Methodology: FA, MB, RC, MO, SE, LB, MC, DB. Investigation: FA, MB, RC, SL, TB, SBé, MO, SBo, MC. Data Curation: FA, MB, RC, SN, MC, DB. Visualization: FA, MB, RC, SN, MC, DB. Funding acquisition: LB, MC, DB. Project administration: MC, DB. Supervision: MC, DB. Writing original draft: SN. Writing review and editing: FA, MB, RC, MO, LB, SN, MC, DB.

Funding

This work was supported by France Alzheimer through the project AmpliTAU and by the French National Research Agency (ANR) through the projects LabEx DISTALZ (ANR-11-LABX-01) and TauSEED (ANR-21-CE18-0046). LilNCog is also supported by LiCEND (Lille Centre of Excellence in Neurodegenerative Disorders), the Métropole Européenne de Lille and the Région Hauts de France.

Data availability

All data needed to evaluate the conclusions in the paper are present in the paper/and or in the Supplementary Materials.

Declarations

Ethics approval and consent to participate

The animal experimental research was performed with the approval of an ethics committee (agreement APAFIS#43474-2023050714441306 from CEEA75, Lille, France) and follows European guidelines for the use of animals. Studies involving human brains were performed in accordance with the ethical standards laid down in the 1964 declaration of Helsinki and its later amendments. Informed consent for tissue donation for research was obtained by the Lille Neurobank (fulfilling French legal requirements concerning

biological resources and declared to the competent authority under the number DC-2008-642) and the Brain Bank Neuro-CEB declared at the Ministry of Higher Education and Research (agreement AC-2018-3290) under their approval procedures. Human samples from the Lille Neurobank were managed by the CRB/CIC1403 Biobank, BB-0033-00030.

Consent for publication
Not applicable.

Competing interests
The authors declare no competing interests.

Received: 3 February 2026 / Accepted: 5 June 2026
Published online: 14 August 2026

References

1. Colin M, Dujardin S, Schraen-Maschke S, Meno-Tetang G, Duyckaerts C, Courade JP et al (2020) From the prion-like propagation hypothesis to therapeutic strategies of anti-tau immunotherapy. Acta Neuropathol 139:3–25. https://doi.org/10.1007/s00401-019-02087-9
2. Jucker M, Walker LC (2013) Self-propagation of pathogenic protein aggregates in neurodegenerative diseases. Nature 501:45–51. https://doi.org/10.1038/nature12481
3. Fitzpatrick AWP, Falcon B, He S, Murzin AG, Murshudov G, Garringer HJ et al (2017) Cryo-EM structures of tau filaments from Alzheimer's disease. Nature 547:185–190. https://doi.org/10.1038/nature23002
4. Falcon B, Zhang W, Murzin AG, Murshudov G, Garringer HJ, Vidal R et al (2018) Structures of filaments from Pick's disease reveal a novel tau protein fold. Nature 561:137–140. https://doi.org/10.1038/s41586-018-0454-y
5. Shi Y, Zhang W, Yang Y, Murzin AG, Falcon B, Kotecha A et al (2021) Structure-based classification of tauopathies. Nature 598:359–363. https://doi.org/10.1038/s41586-021-03911-7
6. Rizzu P, Joosse M, Ravid R, Hoogeveen A, Kamphorst W, van Swieten JC et al (2000) Mutation-dependent aggregation of tau protein and its selective depletion from the soluble fraction in brain of P301L FTDP-17 patients. Hum Mol Genet 9:3075–3082. https://doi.org/10.1093/hmg/9.20.3075
7. Miyasaka T, Morishima-Kawashima M, Ravid R, Kamphorst W, Nagashima K, Ihara Y (2001) Selective deposition of mutant tau in the FTDP-17 brain affected by the P301L mutation. J Neuropathol Exp Neurol 60:872–884. https://doi.org/10.1093/jnen/60.9.872
8. Fairfoul G, McGuire LI, Pal S, Ironside JW, Neumann J, Christie S et al (2016) Alpha-synuclein RT-QuIC in the CSF of patients with alpha-synucleinopathies. Ann Clin Transl Neurol 3:812–818. https://doi.org/10.1002/acn3.338
9. Shahnawaz M, Tokuda T, Waragai M, Mendez N, Ishii R, Trenkwalder C et al (2017) Development of a biochemical diagnosis of Parkinson disease by detection of alpha-synuclein misfolded aggregates in cerebrospinal fluid. JAMA Neurol 74:163–172. https://doi.org/10.1001/jamaneurol.2016.4547
10. Groveman BR, Orru CD, Hughson AG, Raymond LD, Zanusso G, Ghetti B et al (2018) Rapid and ultra-sensitive quantitation of disease-associated alpha-synuclein seeds in brain and cerebrospinal fluid by alphaSyn RT-QuIC. Acta Neuropathol Commun 6:7. https://doi.org/10.1186/s40478-018-0508-2
11. Nicot S, Verchere J, Belondrade M, Mayran C, Betemps D, Bougard D et al (2019) Seeded propagation of alpha-synuclein aggregation in mouse brain using protein misfolding cyclic amplification. FASEB J 33:12073–12086. https://doi.org/10.1096/fj.201900354R
12. Saijo E, Ghetti B, Zanusso G, Oblak A, Furman JL, Diamond MI et al (2017) Ultrasensitive and selective detection of 3-repeat tau seeding activity in Pick disease brain and cerebrospinal fluid. Acta Neuropathol 133:751–765. https://doi.org/10.1007/s00401-017-1692-z
13. Kraus A, Saijo E, Metrick MA, Newell K, Sigurdson CJ, Zanusso G et al (2019) Seeding selectivity and ultrasensitive detection of tau aggregate conformers of Alzheimer disease. Acta Neuropathol 137:585–598. https://doi.org/10.1007/s00401-018-1947-3
14. Metrick MA, Ferreira NDC, Saijo E, Kraus A, Newell K, Zanusso G et al (2020) A single ultrasensitive assay for detection and discrimination of tau aggregates of Alzheimer and Pick diseases. Acta Neuropathol Commun 8:22. https://doi.org/10.1186/s40478-020-0887-z
15. Saijo E, Metrick MA, Koga S, Parchi P, Litvan I, Spina S et al (2020) 4-Repeat tau seeds and templating subtypes as brain and CSF biomarkers of frontotemporal lobar degeneration. Acta Neuropathol 139:63–77. https://doi.org/10.1007/s00401-019-02080-2
16. Scialo C, Tran TH, Salzano G, Novi G, Caponnetto C, Chio A et al (2020) TDP-43 real-time quaking induced conversion reaction optimization and detection of seeding activity in CSF of amyotrophic lateral sclerosis and frontotemporal dementia patients. Brain Commun 2:fcaa142. https://doi.org/10.1093/braincomms/fcaa142
17. Vizziello M, Dellarole IL, Ciullini A, Pascuzzo R, Lombardo A, Bellandi F et al (2025) TDP-43 seeding activity in the olfactory mucosa of patients with amyotrophic lateral sclerosis. Mol Neurodegener 20:49. https://doi.org/10.1186/s13024-025-00833-0
18. Groveman BR, Raymond GJ, Campbell KJ, Race B, Raymond LD, Hughson AG et al (2017) Role of the central lysine cluster and scrapie templating in the transmissibility of synthetic prion protein aggregates. PLoS Pathog 13:e1006623. https://doi.org/10.1371/journal.ppat.1006623
19. Raymond GJ, Race B, Orru CD, Raymond LD, Bongianni M, Fiorini M et al (2020) Transmission of CJD from nasal brushings but not spinal fluid or RT-QuIC product. Ann Clin Transl Neurol 7:932–944. https://doi.org/10.1002/acn3.51057
20. Castilla J, Saa P, Hetz C, Soto C (2005) In vitro generation of infectious scrapie prions. Cell 121:195–206. https://doi.org/10.1016/j.cell.2005.02.011
21. Castilla J, Morales R, Saa P, Barria M, Gambetti P, Soto C (2008) Cell-free propagation of prion strains. EMBO J 27:2557–2566. https://doi.org/10.1038/emboj.2008.181
22. Belondrade M, Jas-Duval C, Nicot S, Bruyere-Ostells L, Mayran C, Herzog L et al (2020) Correlation between bioassay and protein misfolding cyclic amplification for variant creutzfeldt-jakob disease decontamination studies. mSphere. https://doi.org/10.1128/mSphere.00649-19
23. Martinez-Valbuena I, Tartaglia MC, Fox SH, Lang AE, Kovacs GG (2024) Four-repeat Tau seeding in the skin of patients with progressive supranuclear palsy. JAMA Neurol 81:1228–1230. https://doi.org/10.1001/jamaneurol.2024.3162
24. Wang Z, Wu L, Gerasimenko M, Gilliland T, Shah ZSA, Lomax E et al (2024) Seeding activity of skin misfolded tau as a biomarker for tauopathies. Mol Neurodegener 19:92. https://doi.org/10.1186/s13024-024-00781-1
25. Leroy K, Bretteville A, Schindowski K, Gilissen E, Authelet M, De Decker R et al (2007) Early axonopathy preceding neurofibrillary tangles in mutant tau transgenic mice. Am J Pathol 171:976–992. https://doi.org/10.2353/ajpath.2007.070345
26. Holmes BB, Furman JL, Mahan TE, Yamasaki TR, Mirbaha H, Eades WC et al (2014) Proteopathic tau seeding predicts tauopathy in vivo. Proc Natl Acad Sci U S A 111:E4376–E4385. https://doi.org/10.1073/pnas.1411649111
27. Benderradji H, Kraiem S, Courty E, Eddarkaoui S, Bourouh C, Faivre E et al (2022) Impaired glucose homeostasis in a tau knock-in mouse model. Front Mol Neurosci 15:841892. https://doi.org/10.3389/fnmol.2022.841892
28. Tucker KL, Meyer M, Barde YA (2001) Neurotrophins are required for nerve growth during development. Nat Neurosci 4:29–37. https://doi.org/10.1038/82868
29. Caillierez R, Begard S, Lecolle K, Deramecourt V, Zommer N, Dujardin S et al (2013) Lentiviral delivery of the human wild-type tau protein mediates a slow and progressive neurodegenerative tau pathology in the rat brain. Mol Ther 21:1358–1368. https://doi.org/10.1038/mt.2013.66
30. Dujardin S, Lecolle K, Caillierez R, Begard S, Zommer N, Lachaud C et al (2014) Neuron-to-neuron wild-type tau protein transfer through a trans-synaptic mechanism: relevance to sporadic tauopathies. Acta Neuropathol Commun 2:14. https://doi.org/10.1186/2051-5960-2-14
31. Danis C, Dupre E, Zejneli O, Caillierez R, Arrial A, Begard S et al (2022) Inhibition of tau seeding by targeting tau nucleation core within neurons with a single domain antibody fragment. Mol Ther 30:1484–1499. https://doi.org/10.1016/j.ymthe.2022.01.009
32. Taniguchi-Watanabe S, Arai T, Kametani F, Nonaka T, Masuda-Suzukake M, Tarutani A et al (2016) Biochemical classification of tauopathies by immunoblot, protein sequence and mass spectrometric analyses of sarkosyl-insoluble and trypsin-resistant tau. Acta Neuropathol 131:267–280. https://doi.org/10.1007/s00401-015-1503-3
33. Mays CE, Yeom J, Kang HE, Bian J, Khaychuk V, Kim Y et al (2011) In vitro amplification of misfolded prion protein using lysate of cultured cells. PLoS ONE 6:e18047. https://doi.org/10.1371/journal.pone.0018047
34. Yokoyama T, Takeuchi A, Yamamoto M, Kitamoto T, Ironside JW, Morita M (2011) Heparin enhances the cell-protein misfolding cyclic amplification efficiency of variant Creutzfeldt-Jakob disease. Neurosci Lett 498:119–123. https://doi.org/10.1016/j.neulet.2011.04.072

35. Moudjou M, Chapuis J, Mekrouti M, Reine F, Herzog L, Sibille P et al (2016) Glycoform-independent prion conversion by highly efficient, cell-based, protein misfolding cyclic amplification. Sci Rep 6:29116. https://doi.org/10.1038/srep29116
36. Albert M, Mairet-Coello G, Danis C, Lieger S, Caillierez R, Carrier S et al (2019) Prevention of tau seeding and propagation by immunotherapy with a central tau epitope antibody. Brain 142:1736–1750. https://doi.org/10.1093/brain/awz100
37. Oosterlynck M, Leroux E, Namasivayam B, Bouillet T, Caillierez R, Loyens A et al (2025) Stratification of brain-derived extracellular vesicles of Alzheimer's disease patients indicates a unique proteomic content and a higher seeding capacity of small extracellular vesicles. Transl Neurodegener 14:63. https://doi.org/10.1186/s40035-025-00519-z
38. Jeganathan S, Hascher A, Chinnathambi S, Biernat J, Mandelkow EM, Mandelkow E (2008) Proline-directed pseudo-phosphorylation at AT8 and PHF1 epitopes induces a compaction of the paperclip folding of Tau and generates a pathological (MC-1) conformation. J Biol Chem 283:32066–32076. https://doi.org/10.1074/jbc.M805300200
39. Tennant JM, Henderson DM, Wisniewski TM, Hoover EA (2020) RT-QuIC detection of tauopathies using full-length tau substrates. Prion 14:249–256. https://doi.org/10.1080/19336896.2020.1832946
40. Frey B, Holzinger D, Taylor K, Ehrnhoefer DE, Striebinger A, Biesinger S et al (2023) Tau seed amplification assay reveals relationship between seeding and pathological forms of tau in Alzheimer's disease brain. Acta Neuropathol Commun 11:181. https://doi.org/10.1186/s40478-023-01676-w
41. Gorski D, Evans H, Allison T, Barria C, Harrison D, Banerjee V et al (2025) Design and application of a Tau seed amplification assay for screening inhibitors of Tau seeding. Alzheimers Res Ther 17:214. https://doi.org/10.1186/s13195-025-01855-y
42. Carlomagno Y, Manne S, DeTure M, Prudencio M, Zhang YJ, Hanna Al-Shaikh R et al (2021) The AD tau core spontaneously self-assembles and recruits full-length tau to filaments. Cell Rep 34:108843. https://doi.org/10.1016/j.celrep.2021.108843
43. Meyer V, Dinkel PD, Rickman Hager E, Margittai M (2014) Amplification of Tau fibrils from minute quantities of seeds. Biochemistry 53:5804–5809. https://doi.org/10.1021/bi501050g
44. Saborio GP, Permanne B, Soto C (2001) Sensitive detection of pathological prion protein by cyclic amplification of protein misfolding. Nature 411:810–813. https://doi.org/10.1038/35081095
45. Goedert M, Jakes R, Spillantini MG, Hasegawa M, Smith MJ, Crowther RA (1996) Assembly of microtubule-associated protein tau into Alzheimer-like filaments induced by sulphated glycosaminoglycans. Nature 383:550–553. https://doi.org/10.1038/383550a0
46. Kampers T, Friedhoff P, Biernat J, Mandelkow EM, Mandelkow E (1996) RNA stimulates aggregation of microtubule-associated protein tau into Alzheimer-like paired helical filaments. FEBS Lett 399:344–349. https://doi.org/10.1016/s0014-5793(96)01386-5
47. Wilson DM, Binder LI (1997) Free fatty acids stimulate the polymerization of tau and amyloid beta peptides. In vitro evidence for a common effector of pathogenesis in Alzheimer's disease. Am J Pathol 150:2181–2195
48. Bruyere-Ostells L, Verchere J, Betemps D, Almela F, Baron T, Bougard D (2025) Subclinical detection of misfolded alpha-synuclein in the blood of M83 mice. Acta Neuropathol 150:2. https://doi.org/10.1007/s00401-025-02909-z
49. Betemps D, Arsac JN, Nicot S, Canal D, Tlili H, Belondrade M et al (2023) Protease-sensitive and -resistant forms of human and murine alpha-synucleins in distinct brain regions of transgenic mice (M83) expressing the human mutated A53T protein. Biomolecules. https://doi.org/10.3390/biom13121788
50. Manca M, Standke HG, Browne DF, Huntley ML, Thomas OR, Orru CD et al (2023) Tau seeds occur before earliest Alzheimer's changes and are prevalent across neurodegenerative diseases. Acta Neuropathol 146:31–50. https://doi.org/10.1007/s00401-023-02574-0

Publisher's note